(4)

OFFICE OF NAVAL RESEARCH

Contract N00014-90-J-1193

TECHNICAL REPORT No. 1

The Hückel Model for Small Metal Clusters. IV. Orbital Properties and Cohesive Energies for Model Clusters of Up to Several Hundred Atoms

by

D. M. Lindsay, Youqi Wang and Thomas F. George

Prepared for Publication

in

Journal of Cluster Science

Departments of Chemistry and Physics
State University of New York at Buffalo
Buffalo, New York 14260

December 1989

UNCLASSIFIED
SECURITY CLASSIFICATION OF THIS PAGE

REPORT DOCUMENTATION PAGE

Form Approved
OMB No. 0704-0188

1a. REPORT SECURITY CLASSIFICATION Unclassified	1b. RESTRICTIVE MARKINGS
2a. SECURITY CLASSIFICATION AUTHORITY	3. DISTRIBUTION/AVAILABILITY OF REPORT Approved for public release; distribution unlimited
2b. DECLASSIFICATION/DOWNGRADING SCHEDULE	
4. PERFORMING ORGANIZATION REPORT NUMBER(S) UBUFFALO/DC/89/TR-1	5. MONITORING ORGANIZATION REPORT NUMBER(S)
6a. NAME OF PERFORMING ORGANIZATION Depts. Chemistry & Physics State University of New York 6b. OFFICE SYMBOL (If applicable)	7a. NAME OF MONITORING ORGANIZATION
6c. ADDRESS (City, State, and ZIP Code) Fronczak Hall, Amherst Campus Buffalo, New York 14260	7b. ADDRESS (City, State, and ZIP Code) Chemistry Program 800 N. Quincy Street Arlington, Virginia 22217
8a. NAME OF FUNDING/SPONSORING ORGANIZATION Office of Naval Research 8b. OFFICE SYMBOL (If applicable)	9. PROCUREMENT INSTRUMENT IDENTIFICATION NUMBER Contract N00014-90-J-1193
8c. ADDRESS (City, State, and ZIP Code) Chemistry Program 800 N. Quincy Street Arlington, Virginia 22217	10. SOURCE OF FUNDING NUMBERS PROGRAM ELEMENT NO. / PROJECT NO. / TASK NO / WORK UNIT ACCESSION NO.

11. TITLE (Include Security Classification)
The Huckel Model For Small Metal Clusters.IV.Orbital Properties and Cohesive Energies For Model Clusters Of Up To Several Hundred Atoms.

12. PERSONAL AUTHOR(S)
D.M. Lindsay , Youqi Wang , Thomas F. George

13a. TYPE OF REPORT	13b. TIME COVERED	14. DATE OF REPORT (Year, Month, Day)	15. PAGE COUNT
	FROM _____ TO _____	December 1989	34

16. SUPPLEMENTARY NOTATION
Prepared for publication in Journal of Cluster Science

17. COSATI CODES			18. SUBJECT TERMS (Continue on reverse if necessary and identify by block number)	
FIELD	GROUP	SUB-GROUP	METAL CLUSTERS	COHESIVE ENERGIES
			HÜCKEL MODEL	SMALL CLUSTERS
			ORBITAL PROPERTIES	UP TO SEVERAL HUNDRED ATOMS

19. ABSTRACT (Continue on reverse if necessary and identify by block number)

We examine model cluster structures by applying the simple Hückel method to spherically symmetric clusters whose atoms are constrained to occupy cubic (simple, body-centered or face-centered) and hcp lattice positions. The Hückel orbitals are organized into energy shells, many of which remain well separated even at 500-600 atom cluster sizes. The classical droplet model provides a good fit to cluster atomization energies, which then correctly extrapolate to the bulk cohesive energy predicted by tight binding calculations. Energy level distributions for cubic lattices show that features characteristic of a tight binding solid become fully evident in clusters containing as few as 100 atoms. A particular example is the high density of states found for the Fermi level of bcc clusters, vestiges of which might suffice to confer on suitable materials an enhanced electrical conductivity.

20. DISTRIBUTION/AVAILABILITY OF ABSTRACT	21. ABSTRACT SECURITY CLASSIFICATION
☒ UNCLASSIFIED/UNLIMITED ☒ SAME AS RPT. ☐ DTIC USERS	Unclassified
22a. NAME OF RESPONSIBLE INDIVIDUAL Dr. David L. Nelson	22b. TELEPHONE (Include Area Code) (202) 696-4410 / 22c. OFFICE SYMBOL

DD Form 1473, JUN 86 *Previous editions are obsolete.*

SECURITY CLASSIFICATION OF THIS PAGE
UNCLASSIFIED

Journal of Cluster Science, in press

THE HÜCKEL MODEL FOR SMALL METAL CLUSTERS. IV. ORBITAL PROPERTIES AND COHESIVE ENERGIES FOR MODEL CLUSTERS OF UP TO SEVERAL HUNDRED ATOMS.

D. M. Lindsay
Department of Chemistry
City University of New York, The City College
New York, New York 10031

Youqi Wang
Department of Chemistry
California Institute of Technology
Pasadena, California 91125

Thomas F. George
Departments of Chemistry and Physics & Astronomy
State University of New York at Buffalo
Buffalo, New York 14260

ABSTRACT

We examine model cluster structures by applying the simple Hückel method to spherically symmetric clusters whose atoms are constrained to occupy cubic (simple, body-centered or face-centered) and hcp lattice positions. The Hückel orbitals are organized into energy shells, many of which remain well separated even at 500-600 atom cluster sizes. The classical droplet model provides a good fit to cluster atomization energies, which then correctly extrapolate to the bulk cohesive energy predicted by tight binding calculations. Energy level distributions for cubic lattices show that features characteristic of a tight binding solid become fully evident in clusters containing as few as 100 atoms. A particular example is the high density of states found for the Fermi level of bcc clusters, vestiges of which might suffice to confer on suitable materials an enhanced electrical conductivity.

I. INTRODUCTION

While the two extrema, the free atom and the bulk metal, are quite well understood, much less is known about the transition region in between. The passage from an atom to bulk material might be envisaged as occurring in roughly three stages. Molecular size clusters, containing from two to perhaps as many as 50 atoms, will have properties that are noticeably dependent upon geometry. In some ill defined region, geometrical features are no longer paramount and cluster properties will be decided by a combination of lattice structure (not necessarily that of the bulk) and surface effects. For very large aggregates, neither geometry nor the surface will be particularly important and these species will be nearly indistinguishable from a macroscopic sample. The current interest surrounding metal cluster research (which can be traced to the earliest days of computational chemistry)[1] derives in large part from the challenge of unravelling the factors which most influence the first two stages in the transition to a bulk material.

One experimental approach (adopted mainly by chemists) is to start with the atom and then synthesize progressively larger cluster sizes, attempting to find the "onset" of bulk properties such as band structure,[2] metallic properties,[3] plasma resonances,[4] ionization behavior,[5-8] orbital composition,[9] etc. A second method (more favored by physicists) involves growing increasingly smaller particles and looking for the appearance of "quantum size" effects in, for example, their magnetic or thermodynamic properties.[10] Although in principle complementary, the latter approach is difficult for particles less than 20 Å in diameter, while the molecular measurements are usually performed on clusters which contain at most 100 atoms. There exists a similar and perhaps more severe dichotomy in the computational treatment of metal clusters. In general,[11] cluster calculations subdivide into two

classes: detailed, often *ab-initio*, studies on clusters containing 2-13 atoms[12] and less refined surveys of 10 ~ 100 atom aggregates.[13,14] At the other extreme, the electronic properties of bulk metals have been characterized by a variety of theoretical techniques such as sophisticated tight binding calculations,[15] cellular methods,[16] augmented plane waves,[16] density functional methods,[17,18] etc. Quite naturally, there have been few attempts (outside of an occasional foray)[19-21] to extend molecular structure techniques to hundreds or thousands of atoms, nor (excepting density functional treatments)[22-26] are solid state methods easily applied to large, but finite, systems.

In three earlier papers,[27-29] we have shown that Hückel molecular orbital (HMO) calculations will predict reasonable structures and binding energies for small alkali-like metal clusters. M_2-M_{14}. It is not possible, however, to perform a rigorous search for the most stable geometries of clusters containing more than about 10 atoms. In this paper we investigate *model* cluster structures with the aim of extending some of our earlier observations and also of exploring the gap between the molecular and solid state regimes. Akin to the ideas of a "cubium" model,[20,21] we have applied the simple Hückel technique to spherically symmetric clusters whose atoms are constrained to occupy simple cubic (sc), body-centered cubic (bcc), face-centered cubic (fcc) and hexagonal close packing (hcp) lattice positions. Aside from the ease of treating clusters containing several hundred atoms, this approach has the advantage of having a well defined limit, namely the tight binding model (TBM),[30-33] for an infinite array of atoms. The calculations are restricted (for the most part) to nearest neighbor bonding interactions (and so a unique bond length) which precludes a meaningful comparison with the icosahedral structure, even though this arrangement may be quite stable.[34] While obviously unrealistic for molecular size clusters, the assumption of a definite lattice structure may not be as significant a re-

striction for clusters containing several hundred atoms. A more serious question relates to the applicability of simple tight binding calculations. As just noted, the HMO model gives surprisingly good results for both neutral and ionic clusters and can even (in certain aspects) be *correctly* extrapolated to infinite cluster size. However, the simple TBM is a poor predictor of bulk behavior. Accordingly, our Hückel results for 1 ~ 500 atom clusters may (as discussed below) be quantitatively misleading, although we believe they do give considerable qualitative insight into the transition to bulk behavior.

II. SPHERICAL CLUSTERS HAVING CRYSTAL SYMMETRIES

The position of an atom (or group of atoms) in a cubic or hcp crystal can be specified by a linear combination

$$\mathbf{r} = n_1\mathbf{a}_1 + n_2\mathbf{a}_2 + n_3\mathbf{a}_3 + n_4\mathbf{a}_4 \qquad (1)$$

of primitive vectors $\mathbf{a}_i$ (i = 1-3) where the expansion coefficients (n_i) are constrained to be integral.[30-33] Differing Bravais lattices may be defined through different sets of $\mathbf{a}_i$ expressed in terms of orthogonal, unit vectors $\hat{x}$, $\hat{y}$ and $\hat{z}$ and a lattice constant, a. Table I summarizes these relationships for the three cubic lattices and for the hcp arrangement. For hcp, the displacement vector $\mathbf{a}_4$ specifies the relationship between two interpenetrating simple hexagonal lattices and n_4 is either 0 or 1.[31] Table I also gives lattice constants expressed in terms of a "Hückel unit" (abbreviated to hu) of distance. The latter is defined by setting the distance between *nearest neighbor* atoms equal to unity.

For an infinite array of atoms, there are no restrictions on the magnitudes of the integers (n_1, n_2, n_3). For a metal (or other) *cluster*, constrained to have the symmetry

of a particular crystal lattice, then Eq. (1) still pertains but now the n_i have maximum values determined by the finite cluster radius. Spherically symmetric clusters can be generated by finding all sets of n_i for which r is less than a chosen maximum radius. In the case of a simple cubic lattice, for example, then Eq. (1) together with the data of Table I gives (distances in hu)

$$r^2 = I = n_1^2 + n_2^2 + n_3^2$$
$$I = 0, 1, 2, 3, ..., M \qquad (2).$$

where M (which is an integer) corresponds to the maximum cluster radius. Appendix A outlines the algorithm used for generating integral n_i subject to the constraints of Eq. (2). Table II gives the shell radii and atomic occupations[35] for simple cubic clusters having up to 23 shells. Each shell may be characterized by an integral shell number, where shell number 0 pertains to the central atom. Shell number 1 contains 6 additional atoms whose integer "co-ordinates" are $(n_1, n_2, n_3) = (0, 0, \pm1)$, $(0, \pm1, 0)$ and $(\pm1, 0, 0)$ and so forth. Notice that not every r^2 equal to an integer will generate integral n_i. Thus, for example, there is no Table II entry under $r^2 = 7$ in the case of a simple cubic lattice. Accordingly, there is not a 1-1 correspondence between the integer I and the shell number. Analogous to the simple cubic case, shell radii for bcc, fcc and hcp structures are defined by the relations

$$3r^2 = I = n_1^2 + n_2^2 + n_3^2 - 2(n_1n_2 + n_1n_3 + n_2n_3)$$
$$I = 0, 1, 2, ..., 3M \qquad (3)$$

$$r^2 = I = n_1^2 + n_2^2 + n_3^2 + n_1n_2 + n_1n_3 + n_2n_3$$
$$I = 0, 1, 2, ..., M \qquad (4)$$

$$3r^2 = I = 3(n_1^2 + n_2^2 + n_4^2) + 8n_3^2 + 3(n_1n_2 + n_1n_4 + n_2n_4) + 8n_3n_4$$
$$I = 0, 1, 2, ..., 3M \qquad (5)$$

respectively. Appendix A also gives algorithms for computing n_i satisfying Eqs. (3), (4) or (5). Table II summarizes the shell radii and atomic occupation numbers[35] for the four lattice structures considered in this paper.

The Hückel matrix for an n atom cluster has matrix elements given by ($1 \leq i \neq j \leq n$):

$$H_{ii} = \alpha$$
$$H_{ij} = \begin{cases} -\beta \text{ if i is bonded to j} \\ 0 \text{ otherwise} \end{cases} \qquad (6)$$

where α and β denote the empirical Hückel Coulomb and resonance integrals, respectively. As in previous work,[27-29] we choose energy units in which $\alpha = 0$ and $\beta = 1$ and denote these "Hückel units", abbreviated to hu. We have not attempted to adjust the Hückel β-parameter for either cluster size or atomic coordination number. While global properties, such as cluster cohesive energies, are relatively insensitive to small variations of this sort,[25,36,37] an invariant β may preclude an accurate description of certain surface effects.[21]

It is relatively straightforward to generate the Hückel matrix from the previously computed integers, n_i. The criterion for i to be bonded to j is simply $|r(i) - r(j)| = 1$, where in the case of sc clusters, for example, the distance between two atoms (i and j) is given by

$$| \mathbf{r}(i) - \mathbf{r}(j) |^2 = [n_1(i) - n_1(j)]^2 + [n_2(i) - n_2(j)]^2 + [n_3(i) - n_3(j)]^2$$

and similar, but more complicated expressions pertain to the bcc, fcc and hcp arrangements. The eigenvalues (ε_i) and eigenfunctions were obtained by numerical diagonalization of Hückel matrices containing up to 555 atoms. In order to obtain well defined electron distributions, symmetry adapted wavefunctions which transform as irreducible representations of the O_h point group were constructed using projection operator techniques. The atomization energy of an n atom cluster is given by

$$\Delta E(n) = \sum_i m_i \varepsilon_i \qquad (7)$$

$$n = \sum_i m_i$$

where the summations extend over all occupied ($m_i = 2$) or partially occupied ($m_i = 1$) molecular orbitals.

III. DISCUSSION

A. Cluster cohesive energies

Table III gives $\Delta E(n)/n$, the cluster atomization energy per atom, for sc, bcc and fcc clusters having up to 22 atomic shells. Also given in this table are the corresponding bulk parameters, namely the crystal cohesive energies. The latter were calculated numerically from [38]

$$\Delta E(n)/n = \frac{2}{(2\pi)^3} \iiint_{\varepsilon(\mathbf{k}) \le E_f} \varepsilon(\mathbf{k})\, dk_1 dk_2 dk_3 \qquad (8)$$

with

$$\varepsilon(\mathbf{k}) = -2\{\cos k_1 + \cos k_2 + \cos k_3\} \qquad (9)$$

or
$$\varepsilon(\mathbf{k}) = -2\{\cos k_1 + \cos k_2 + \cos k_3 + \cos(k_1 + k_2 + k_3)\} \qquad (10)$$

or
$$\varepsilon(\mathbf{k}) = -2\{\cos k_1 + \cos k_2 + \cos k_3 + \cos(k_1 - k_2) + \cos(k_1 - k_3) + \cos(k_2 - k_3)\} \qquad (11)$$

for simple, body-centered and face-centered cubic lattices, respectively. Eqs. (9)-(11) are special cases of the more general result[30-33]

$$\varepsilon(\mathbf{k}) = \alpha - \beta \sum_{nn} e^{i\mathbf{k}\cdot\mathbf{r}} \qquad (12)$$

which gives the tight binding eigenvalues when only nearest neighbor (nn) interactions are included. In these expressions, k is the electron wavevector written in terms of reciprocal lattice basis vectors

$$\mathbf{k} = k_1\mathbf{b}_1 + k_2\mathbf{b}_2 + k_3\mathbf{b}_3 \qquad (13)$$

where the $\mathbf{b}_i$ are defined in terms of the previously introduced (see Eq. (1) and Table I) primitive vectors $\mathbf{a}_1$, $\mathbf{a}_2$ and $\mathbf{a}_3$ by [39]

$$\mathbf{a}_i \cdot \mathbf{b}_j = \delta_{ij} \qquad (14).$$

Cohesive energies were evaluated by subdividing the first Brillouin zone ($-\pi \leq k_i \leq +\pi$) into small volume elements which contribute to the integral in Eq. (8) only if $\varepsilon(\mathbf{k})$, as given by Eqs. (9), (10) or (11), is less than the crystal Fermi energy, E_f.

Figure 1 shows plots of $\Delta E(n)/n$ versus n for bcc and fcc clusters. The atomization energies for simple cubic clusters fall close to the bcc data points and were omitted for clarity. The full lines in this figure are least squares fits of the Table III data to the liquid drop expression

$$\Delta E(n)/n = A + Bn^{-1/3} \qquad (15)$$

where the A and B terms pertain to volume and "surface" energy contributions, respectively.[28,40] For small bcc (and sc) clusters, the HMO atomization energies deviate noticeably from the classical curve. For $n \geq 100$, where geometrical features are no longer paramount, these quantum oscillations become much smaller and $\Delta E(n)/n$ converges smoothly and slowly to its asymptotic value. For a 600 atom bcc cluster, for example, $\Delta E(n)/n$ is approximately 85% of its bulk value. Only after 10-20,000 atoms will bcc clusters acquire 95% of their bulk cohesive energy. The atomization energies of fcc and hcp clusters show a less oscillatory behavior, as (perhaps unexpectedly) do the less symmetric M_2 - M_{14} clusters. The extent of the deviations from classical behavior at small n appears to correlate with the number of bonding neighbors. Thus, with a next nearest neighbor interaction included (see below), the bcc oscillations become noticeably less pronounced. The A parameter in Eq. (15) represents the cohesive energy of the bulk crystal, obtained by extrapolating from finite crystal sizes to infinity. Table IV gives the best fit A and B parameters with one standard deviation uncertainty in parentheses.[41] Table IV also compares A coefficients with the previously discussed "exact" cohesive energies obtained from Eq. (8). The two data sets differ by <10%, which implies that cluster atomization energies are in-

deed well represented by a liquid drop model. As in several previous examples,[28] the classical A and B parameters are similar in their magnitudes, thus ensuring that the "critical nucleus",[42] $n^* = (-2B/3A)^3$, is always less than unity.

Fig. 1 also shows the liquid drop curve (data points omitted for clarity) obtained from the HMO atomization energies of the *most stable* neutral clusters, M_2-M_{14}. As discussed in Ref. 28, these data predict a bulk cohesive energy of 3.0(1)β. Furthermore, with an appropriate choice of the Hückel β-parameter, extrapolated HMO cohesive energies differ, on average, by only 15% from the experimental values for Li → Cs.[28] Since simple Hückel calculations also give *cluster* atomization energies in good agreement with experiment and *ab-initio* theory,[28] the curve denoted M_2-M_{14} in Fig. 1 is, presumably, a fairly accurate representation of $\Delta E(n)/n$ for the Group IA elements at all $2 \leq n \leq \infty$. Thus, although the crystal structure of the alkali metals is body-centered cubic, the Hückel data for spherical bcc clusters significantly underestimates atomization energies, even at the bulk limit. This is not totally surprising, since simple tight binding calculations are known to be erroneous in several of their predictions (see below) for the alkali metals. Figure 1 shows that simple Hückel calculations predict fcc (and hcp)[43] clusters to be much more stable than the body-centered arrangement, apparently because there are four additional nearest neighbors in the former. The atomization energies of hcp and fcc clusters are very similar. As can be seen from Table II, the two structures become distinguishable only when third nearest neighbor atoms are considered.[44] However, bcc clusters have six *next* nearest neighbors (see Table II) which are only 15% more distant than the nearest neighbor shell and so bcc and fcc packing fractions differ by only 6%.[22,45] This suggests that including the bonding of next nearest neighbor atoms would improve the relative stability of bcc clusters and might in addition give better cohesive energies for the bulk bcc solid. In fact, HMO calculations which do include a next nearest neighbor

interaction (γ, in units of β) show that bcc atomization energies increase for all $0 \leq \gamma \leq 1$. However, even if γ is close to unity, asymptotic cohesive energies are still significantly smaller than 3.0β.[46]

B. Hückel energy levels

Figure 2 summarizes the positions of the Hückel orbital energies (denoted by horizontal tick marks) for cubic and hcp lattices. Since Hückel theory is the molecular analog of the tight binding model (TBM) for a macroscopic sample, the overall appearance of these plots reflects the band structure predicted by tight binding calculations. Thus (see also section III.C) the eigenvalue spectra for sc and bcc lattices are symmetric about the atomic energy ($\alpha = 0$), with extrema at $\pm 6\beta$ and $\pm 8\beta$, respectively, where the lower bound is identically equal to the number of nearest neighbors in the lattice. For all $n = 1 - \infty$, the Fermi level lies at precisely 0 hu. In the case of fcc and hcp, however, the bulk state distributions are asymmetric: the TBM energies lie between -12β and $+4\beta$ and the Fermi energy is slightly greater than 0 hu.

In contrast to the bulk case, finite clusters have a finite number of energy levels. As shown in Fig. 2 these energies are organized into well defined shells which, as described elsewhere,[28,47] may be classified by the global nodal character of the cluster wavefunctions. Thus, for example, the lowest cluster orbital has no angular or radial nodes and so can be denoted 1s. The wavefunctions for the next lowest cluster eigenvalue, whose three fold degeneracy[48] is not shown in Fig. 2, have one angular node and so correspond to three orthogonal 1p orbitals. Following 1p, cluster orbitals group by energy as 1d, 2s and 1f. However, the 1d and 1f degeneracies are partially lifted, the extent of this being dependent upon cluster size. The appearance of energy shells is a natural consequence of quantum (notably jellium) models in

which the electrons are assumed to move in a spherically symmetric potential arising from a *uniform* background of positive charge.[6,22-24,49,50] In a previous Hückel study of molecular clusters (whose atoms were *not* constrained to have crystal symmetry) it was shown that filled, cluster orbitals were organized into well separated energy shells, and that these could be parameterized to give results similar to those obtained by conventional jellium calculations.[28] It is not surprising, therefore, that the highly symmetric model structures considered here should also show shell structures. What is notable is the *persistence* of the energy shells, even for clusters containing 500-600 atoms. For a 537 atom sodium cluster having a bcc structure, for example, the 1s-1p gap is still 0.2 eV,[51] and will fall below 0.1 eV (fitting the 1s and 1p shell energies to expressions similar to Eq. (2) of Ref. 28)[52] only for clusters containing over 2000 atoms.

C. Density of states

Figure 3 shows the density of states (DOS) for selected cluster sizes and also makes a comparison with the bulk solid. The histograms for $n \approx 100$, 250 and 500 were derived by dividing the total range of allowed eigenvalues (16 hu) into equal increments ($\Delta\varepsilon$) and then counting the number, $g_n(\varepsilon)$, of states (*including* degeneracies) within each section. The data shown in Fig. 3 pertain to $g_n(\varepsilon)$ in units of states/hu for $\Delta\varepsilon = 16 \div 33$ hu. We chose this $\Delta\varepsilon$ (which is somewhat arbitrary) in order to "smooth out" some of the shell structure shown in Fig. 2, as this makes a comparison with the bulk DOS profiles more compelling.

For an infinite crystalline solid, the density of states per unit volume may be evaluated from[30-33]

$$g(\varepsilon) = \frac{2}{a^3 V} \int\int \frac{dS}{|\nabla \varepsilon|} \qquad (16)$$

where S is a surface of constant energy in k-space, $\nabla\varepsilon$ is the energy gradient normal to this surface, V is the volume of the first Brillouin zone ($8\pi^3/a^3$, $16\pi^3/a^3$ and $32\pi^3/a^3$ for sc, bcc and fcc lattices, respectively)[32] and the factor of two accounts for electron spin degeneracy. The density of states derived from tight binding calculations is well known and results for sc and bcc lattices are shown in, for example, Fig. 38 of Ref. 33. We re-evaluated $g(\varepsilon)$ by numerically integrating Eq. (16), but using instead of Eqs. (10) and (11) tight binding eigenvalues expressed in terms of k_x, k_y and k_z,[53] and our computed DOS profiles are given in Figures 3a and 3b. For fcc lattices (Fig. 3c), where the integration limits are more difficult to visualize, we employed Eq. (11) and evaluated $g(\varepsilon)$ by counting the number of points in k-space lying within two concentric surfaces of constant and nearly equal energy. Also shown in Fig. 3c is the Fermi energy for an fcc lattice, E_f = 0.459 hu. This parameter equals the energy at which the tight binding orbitals are exactly half filled, and was determined by numerical integration of the computed $g(\varepsilon)$ versus ε data. As noted earlier, E_f = 0 hu for both sc and bcc lattices.

The most noticeable feature of Fig. 3 is the close similarity between the state densities of relatively small clusters and bulk materials. This is particularly striking for the symmetric sc and bcc profiles, from which it is apparent that most of the features of the bulk DOS are evident in clusters containing 100 (or fewer) atoms. The "discontinuities" (van Hove singularities)[30,31] in the bulk curves occur at points where the Fermi surface comes into contact with the first Brillouin zone and so the form of the bulk DOS is particularly dependent upon the shapes of these two surfaces. Thus the data shown in Fig. 3 imply that small metal clusters have both an in-

cipient Fermi surface and a nascent Brillouin zone structure, although neither "surface" would (of course) be continuous.

The tight binding model predicts an infinite, but integrable, density of states at the Fermi level (E_f = 0 hu) of a bcc solid.[33] As shown in Fig. 3b, the corresponding cluster phenomenon is an extremely high value for the degeneracy, $D_n(\varepsilon)$, of the Hückel orbitals at ε = 0 hu. The actual Fermi level degeneracy, given in Table V, increases (fairly systematically)[54] with increasing cluster size. The *fractional* Fermi level degeneracy, $D_n(0)/n$ given in column 4 of Table V, decreases rather slowly so that (for example) 15% of the Hückel orbitals in a 500 atom bcc cluster are located at ε = 0 hu. The Hückel calculations also predict a relatively large Fermi level degeneracy for simple cubic clusters. This degeneracy does not increase regularly with cluster size and is relatively less important than in the bcc case. For example, the 515 atom cluster shown in Fig. 3a has a 25-fold degeneracy at ε = 0, which would be more noticeable if the Fig. 3a data were plotted using a smaller energy increment, $\Delta\varepsilon$. As a corollary of these high degeneracies, large energy gaps appear near to the Fermi level of both sc and bcc clusters. For a 500 atom cluster, the energy level spacing near E_f is $\delta_f \approx$ 500 - 1000 K (we specialize to the case of sodium)[51] which is considerably greater than the comparable quantity[32] for a free electron Fermi gas, $\delta_f \approx 3E_f/4n \approx$ 40K.[55] Accordingly, alkali-like metal clusters might show measurable quantum size effects[10] for much larger sizes than those predicted by the simple Kubo criterion $\delta_f \approx kT$,[56] even if these aggregates are less symmetric than the idealized structures considered here.

IV. CONCLUSION

In concluding, we re-emphasize that our calculations pertain to *model* cluster structures. Our objective has been to expand upon some earlier observations,[27-29] in particular the connection between molecular orbital calculations and simpler, but valid, descriptions such as the shell and liquid drop models. In addition, we wanted to explore theoretically the relationship between cluster and bulk properties (cohesive energies, state densities, etc.) under conditions where the two extrema are well defined. Actual systems are unlikely to be so agreeable. Thus, for example, a real cluster of several hundred alkali atoms, even if approximately body-centered cubic, would presumably show only a vestige of the degeneracy predicted by Table V and Fig. 3b.

A more serious criticism of the Hückel model lies in the well known failure of tight binding calculations to correctly predict certain features of real metals. For example, de Haas-van Alphen measurements suggest that the Fermi surface of the alkali metals is nearly a perfect sphere (some deviations from sphericity may exist, however)[57], whereas the TBM predicts pronounced "neck-like" features.[31] Thus, the bulk metal is better described by a Fermi gas model, and this will give DOS profiles quite different from those described above.[33] Since *simple* Hückel calculations are surprisingly reliable for molecular size clusters,[27-29] the source of their poor performance in larger systems is not entirely clear. As noted in Ref. 28, both HMO and tight binding calculations make rather drastic simplifications. In particular, we refer to the neglect of hybridization (a significant factor for alkali clusters)[9] and to the use of single electron wavefunctions. For alkali metals, there is a convenient cancellation of Coulomb and exchange terms and so the latter approximation is actually quite good.[58] Any prediction of absolute orbital and cohesive energies will implicitly

include hybridization (and overlap) effects since the Hückel β-parameter is always chosen from experimental data. However, s-p hybridization will change the character of the Fermi surface, making it in fact more free electron like (e.g. see Sect. II 4 of Ref. 33). As noted earlier, we also tested the effect of next nearest neighbor interactions. In addition to improving cluster binding energies, these should provide a mechanism for further "delocalizing" the valence electrons. For bcc clusters, the inclusion of next nearest neighbor interactions does, in fact, give a DOS profile whose appearance is more like that expected (Compare curves (1), (2) and (3) in Fig. 38 of Ref. 33) for a Fermi gas. Conversely, it is interesting to speculate on the possible existence of bcc materials (cluster or bulk) which *can* be accurately described by a simple tight binding model. Because of the predicted high density of states at E_f, these materials would be expected to have particularly large electrical conductivities and might even be good candidates for high T_c superconductors.

ACKNOWLEDGMENTS

We thank Lin Chu for her assistance in completing the Hückel calculations. TFG acknowledges research support by the Office of Naval Research and the National Science Foundation under Grant No. CHE-8620274. DML acknowledges the support of this work by the National Science Foundation under Grants No. CHE-8307164 and RII-8305241 and by The City University of New York PSC-BHE Faculty Research Award Program.

APPENDIX A: ATOM POSITIONS IN SPHERICAL CLUSTERS

For a cubic or hcp lattice, atomic position vectors may be specified by

$$r = n_1a_1 + n_2a_2 + n_3a_3 + n_4a_4$$

with a_i given in Table I. In a finite cluster whose overall shape is spherical, the integers n_i (i=1-3) are subject to the constraint that r^2 should not exceed a chosen maximum value and $n_4 = 0$ or 1, as described in section II. In order to find these sets of n_i, it is convenient to use the combinations $X = n_1 + n_2$, $Y = n_1n_2$ and $Z = (n_1 + n_2)^2 \geq 0$, so that

$$n_1 = (X \pm \{Z - 4Y\}^{1/2})/2 \qquad \text{(A1)}$$

and

$$n_2 = X - n_1 \qquad \text{(A2)}$$

where integral n_i require $Z \geq 4Y$. Eqs. (2) - (5) in the text give the additional relations

$$n_3 = \pm\{I - (Z - 2Y)\}^{1/2} \qquad \text{(A3)}$$

or

$$n_3 = (X \pm \{3I + 24Y - 8Z\}^{1/2})/3 \qquad \text{(A4)}$$

or

$$n_3 = (-X \pm \{4(I + Y) - 3Z\}^{1/2})/2 \qquad \text{(A5)}$$

or

$$n_3 = 1/4(-2n_4 \pm \{2[I - n_4] + 6[Y - Z - n_4X]\}^{1/2}) \qquad \text{(A6)}$$

for sc, bcc, fcc or hcp lattice structures, respectively. In order that n_3 be integral, the terms in braces must be positive or zero. Combining this requirement with $Z \geq 4Y$ and $Z \geq 0$ gives

$$I = 0, 1, 2, \ldots\ldots, M$$
$$Y = -[I/2], -[I/2] + 1, \ldots\ldots, +[I/2] \qquad \text{(A7)}$$

$$Z = \max(0,4Y), \max(0,4Y) + 1, \ldots\ldots, (I + 2Y)$$

$$\begin{aligned} I &= 0, 1, 2, \ldots\ldots, 3M \\ Y &= -[I/8], -[I/8] + 1, \ldots\ldots, +[3I/8] \\ Z &= \max(0,4Y), \max(0,4Y) + 1, \ldots\ldots, [3(I + 8Y)/8] \end{aligned} \qquad \text{(A8)}$$

$$\begin{aligned} I &= 0, 1, 2, \ldots\ldots, M \\ Y &= -I, -I + 1, \ldots\ldots, +[I/2] \\ Z &= \max(0,4Y), \max(0,4Y) + 1, \ldots\ldots, [4(I + Y)/3] \end{aligned} \qquad \text{(A9)}$$

$$\begin{aligned} I &= 0, 1, 2, \ldots\ldots, M \\ \sqrt{Z} &= -[2/3(\sqrt{I}+n_4)], -[2/3(\sqrt{I}+n_4)] + 1, \ldots\ldots, +[2/3(\sqrt{I}-n_4)] \\ Y &= -[I/3], -[I/3] + 1, \ldots\ldots, +[Z/4] \end{aligned} \qquad \text{(A10)}$$

where Eqs. (A7) - (A10) pertain to sc, bcc, fcc and hcp (here $n_4 = 0$ or 1, except for $I = 0$) lattices, respectively, and [N] denotes the integer part of N. Thus, the algorithm we used to generate integer (n_1, n_2, n_3) is: (i) for each I, find possible Y and Z according to Eqs. (A7) - (A10); (ii) if $\sqrt{Z}$ is not an integer, reject the set of I, Y, Z; (iii) if the terms in braces in either Eq. (A2) or the appropriate member of (A3) - (A6) are not integers, reject the set of I, Y, Z; (iv) otherwise, construct n_1, n_2 and n_3 from (A1), (A2) and one of (A3) - (A6).

REFERENCES

1. H. S. Taylor, H. Eyring and A. Sherman, J. Chem. Phys. **1**, 68 (1933).

2. M. Moskovits and J. E. Hulse, J. Chem. Phys. **66**, 3988 (1977); **67**, 4271 (1977); J. Stapelfeldt, J. Wörmer and T. Möller, Phys. Rev. Lett. **62**, 98 (1989).

3. K. Rademann, B. Kaiser, U. Even and F. Hensel, Phys. Rev. Lett. **59**, 2319, (1987); C. Bréchignac, M. Broyer, Ph. Cahuzac, G. Delacretaz, P. Labastie, J. P. Wolf and L. Wöste, Phys. Rev. Lett. **60**, 275, (1988).

4. G. A. Ozin and H. Hüber, Inorg. Chem. **17**, 155 (1978); W. Schulze and H. Abe, Disc. Far. Soc. **14**, 87 (1980); W. Vogel, B. Tesche and W. Schulze, Chem. Phys. **74**, 137 (1983); W.A. de Heer, K. Selby, V. Kresin, J. Masui, M. Vollmer, A. Châtelain and W. D. Knight, Phys. Rev. Lett. **59**, 1805 (1987).

5. M. M. Kappes, M. Schär, P. Radi and E. Schumacher, J. Chem. Phys. **84**, 1863 (1986); M. M. Kappes, Chem. Rev. **88**, 369 (1988) and references cited therein.

6. M. L. Cohen, M. Y. Chou, W. D. Knight and W. A. de Heer, J. Phys. Chem. **91**, 3141 (1987); W. A. de Heer, W. D. Knight, M. Y. Chou and M. L. Cohen, Solid State Physics **40**, 94 (1987) and references cited therein.

7. K. J. Taylor, C. L. Pettiette, M. J. Craycraft, O. Chesnovsky and R. E. Smalley, Chem. Phys. Lett. **152**, 347 (1988); C. L. Pettiette, S. H. Yang, M. J. Craycraft, J. Conceicao, R. T. Laaksonen, O. Chesnovsky and R. E. Smalley, J. Chem. Phys. **88**, 5377 (1988).

8. D. G. Leopold, J. Ho and W. C. Lineberger, J. Chem. Phys. **86**, 1715 (1987).

9. D. A. Garland and D. M. Lindsay, J. Chem. Phys. **78**, 2813 (1983); D. A. Garland and D. M. Lindsay, J. Chem. Phys. **80**, 4761 (1984).

10. For a recent review of quantum shell effects, see: W. P. Halperin, Rev. Mod. Phys. **58**, 533 (1986).

11. There are exceptions. For example, *ab-initio* calculations have been reported for Be clusters as large as Be_{63}. See: L. Pettersson and C. Bauschlicher, Chem. Phys. Lett. **130**, 111 (1986); W. C. Ermler, R. B. Ross, C. W. Kern, R. M. Pitzer and N. W. WinterJ. Phys. Chem. **92**, 3042 (1988).

12. For recent reviews, see: J. Koutecky and P. Fantucci, Chem. Rev. **83**, 539 (1986); T. Halicioglu and C. W. Bauschlicher, Jr., Rep. Prog. Phys. **51**, 883 (1988).

13. For example: R. C. Baetzold, J. Chem. Phys. **68**, 555 (1978); Inorg. Chem. **20**, 118 (1981); Surf. Sci. **106**, 243 (1981). See, also, R. C. Baetzold in *Metal Clusters*, edited by M. Moskovits, Wiley, 1986, chapter 2.

14. For example, see: R. P. Messmer, Surf. Sci. **106**, 225 (1981); A. T. Amos, P. A. Brook and S. A. Moir, J. Phys. Chem. **92**, 733 (1988).

15. D. W. Bullett, Solid State Physics **35**, 129 (1980).

16. J. M. Ziman, Solid State Physics **26**, 1 (1971).

17. P. Hohenburg and W. Kohn, Phys. Rev. **136**, B864 (1964); W. Kohn and L. J. Sham, Phys. Rev. **137**, A1697 (1965).

18. J. Callaway and N. H. March, Solid State Physics **38**, 135 (1984); M. Farjam and H. B. Shore, Phys. Rev. **B37**, 1059 (1988).

19. D. Kalkstein and P. Soven, Surf. Sci. **26**, 85 (1971).

20. R. P. Messmer, Phys. Rev. **B15**, 1811 (1977).

21. G. B. Bachelet, F. Bassani. M. Bourg and A. Julg, J. Phys. **C16**, 4305 (1983).

22. J. L. Martins, R. Car and J. Buttet, Surf. Sci. **106**, 265 (1981).

23. D. E. Beck, Solid State Commun. **49**, 381 (1984).

24. W. Ekardt, Ber. Bunsenges. Phys. Chem. **88**, 289 (1984); Phys. Rev. **B29**, 1558 (1984).

25. M. P. Iniguez, J. A. Alonso and L. C. Balbas, Solid State Commun. **57**, 85 (1986).

26. M. Manninen, Phys. Rev. **B34**, 6886 (1986); Solid State Commun. **59**, 281 (1986).

27. Y. Wang, T. F. George, D. M. Lindsay and A. C. Beri, J. Chem. Phys. **86**, 3493 (1987).

28. D. M. Lindsay, Y. Wang and T. F. George, J. Chem. Phys. **86**, 3500 (1987).

29. D. M. Lindsay, L. Chu, Y. Wang and T. F. George, J. Chem. Phys. **87**, 1685 (1987).

30. J. M. Ziman, *Principles of the Theory of Solids* (Cambridge University, New York, 1972).

31. N. W. Ashcroft and N. D. Mermin, *Solid state Physics* (Saunders, Philadelphia, 1976).

32. C. Kittel, *Introduction to Solid state Physics* (Wiley, New York, 1976).

33. N. F. Mott and H. Jones, *The Theory of the Properties of Metals and Alloys* (Dover, New York, 1958).

34. See, for example: M. B. Gordon, F. Cyrot-Lackmann and M. C. Desjonquerès, Surf. Sci. **80**, 159 (1979); J. W. Lee and G. D. Stein, J. Phys. Chem. **91**, 2450 (1987).

35. More limited sets of shell filling data may be found elsewhere. See, for example, Refs. 22 and 25.

36. D. Tomanek, S. Mukherjee and K. H. Bennemann, Phys. Rev. **B28**, 665 (1983).

37. L. Marville and W. Andreoni, J. Phys. Chem. **91**, 2645 (1987).

38. Analogous expressions are discussed in section 1.6 of Ref. 30.

39. It is customary (e.g. Refs. 30-32) to define $\mathbf{b}_i$ through $\mathbf{a}_i \cdot \mathbf{b}_j = 2\pi\delta_{ij}$. Consequently, our (k_1, k_2, k_3) differ by 2π from their conventional counterparts.

40. The liquid drop model has been most thoroughly discussed in the context of nucleon clusters. See, for example: W. J. Swiatecki, Proc. Phys. Soc. London Ser. A **64**, 226 (1951); W. D. Meyers and W. J. Swiatecki, Nuclear Physics **81**, 1 (1966).

41. The atomic points were not included in the fit of Eq. (15) to the data of Table III.

42. F. A. Abraham, *Homogeneous Nucleation Theory* (Academic, New York, 1974).

43. The liquid drop parameters found for hcp clusters are: A = -2.6(1) , B = 2.0(5).

44. See also Ref. 37.

45. L. Pauling, *The Nature of the Chemical Bond* (Cornell, Ithaca, NY, 1960).

46. Curiously, a small next nearest neighbor interaction *decreases* the stability of fcc clusters. For (implausibly?) larger $\gamma > 0.3$, fcc cluster stabilities increase in magnitude.

47. J. L. Martins, J. Buttet and R. Car, Phys. Rev. **B31**, 1804 (1985).

48. An hcp crystal is not isotropic (i.e. the z direction is not interchangeable with x and y) and, as shown in Fig. 2d, this gives rise to a small, partial lifting of the 1p shell degeneracies.

49. W. D. Knight, K. Clemenger, W. A. de Heer, W. A. Saunders, M. Y. Chou and M. L. Cohen, Phys. Rev. Lett. **52**, 2141 (1984).

50. M. Y. Chou, A. Cleland and M. L. Cohen, Solid State Commun. **52**, 645 (1984).

51. Cluster energies in hu may be converted to eV using β values from Ref. 28. For Na, $\beta = 0.38$ eV.

52. These fits are quite satisfactory and show that the two shells do converge (albeit slowly) in the bulk limit.

53. See, for example: Eqs. (58) in chapter 2 of Ref. 33.

54. The data of Table V show that $D_n(0) = 6m + 1$, where m = 0, 1, 2, etc. However, not all m are covered by the observed sequence of $D_n(0)$, and some m occur more than once.

55. Using n = 500 and $E_f = 3.23$ eV from Ref. 32.

56. R. Kubo, J. Phys. Soc. Japan **17**, 975 (1962); J. de Phys. **C2**, 69 (1977).

57. Y. G. Hwang and A. W. Overhauser, Phys. Rev. **B39**, 3037 (1989).

58. See Sect. IV 2 of Ref. 33 and: A. Haug, *Theoretical Solid State Physics* (Pergamon, New York, 1972).

TABLE I. Relationship between primitive vectors ($\mathbf{a}_1$, $\mathbf{a}_2$, $\mathbf{a}_3$), the displacement vector $\mathbf{a}_4$ and cartesian unit vectors ($\hat{x}$, $\hat{y}$, $\hat{z}$) for cubic and hcp Bravais lattices (see Ref. 31). Bottom row entries are lattice constants (a) in Hückel units (see text).

	sc	bcc	fcc	hcp
$\mathbf{a}_1$	$\hat{x}$	$(\hat{y} + \hat{z} - \hat{x})/\sqrt{3}$	$(\hat{y} + \hat{z})/\sqrt{2}$	$\hat{x}$
$\mathbf{a}_2$	$\hat{y}$	$(\hat{z} + \hat{x} - \hat{y})/\sqrt{3}$	$(\hat{z} + \hat{x})/\sqrt{2}$	$(\hat{x} + \sqrt{3}\hat{y})/2$
$\mathbf{a}_3$	$\hat{z}$	$(\hat{x} + \hat{y} - \hat{z})/\sqrt{3}$	$(\hat{x} + \hat{y})/\sqrt{2}$	$\sqrt{(8/3)}\hat{z}$
$\mathbf{a}_4$	0	0	0	$\mathbf{a}_1/3 + \mathbf{a}_2/3 + \mathbf{a}_3/2$
a	1	$2/\sqrt{3}$	$1/\sqrt{2}$	1

TABLE II. Shell radii and shell occupancies for spherical clusters having cubic or hexagonal close packing lattices. Radii are in hu (see text).

shell number	sc		bcc		fcc		hcp	
	radius	atoms	radius	atoms	radius	atoms	radius	atoms
0	0.000	1	0.000	1	0.000	1	0.000	1
1	1.000	6	1.000	8	1.000	12	1.000	12
2	1.414	12	1.155	6	1.414	6	1.414	6
3	1.732	8	1.633	12	1.732	24	1.633	2
4	2.000	6	1.915	24	2.000	12	1.732	18
5	2.236	24	2.000	8	2.236	24	1.915	12
6	2.449	24	2.309	6	2.449	8	2.000	6
7	2.828	12	2.517	24	2.646	48	2.236	12
8	3.000	30	2.582	24	2.828	6	2.380	12
9	3.162	24	2.828	24	3.000	36	2.449	6
10	3.317	24	3.000	32	3.162	24	2.517	6
11	3.464	8	3.266	12	3.317	24	2.582	12
12	3.606	24	3.416	48	3.464	24	2.646	24
13	3.742	48	3.464	30	3.606	72	2.708	6
14	4.000	6	3.651	24	3.873	48	2.887	12
15	4.123	48	3.786	24	4.000	12	3.000	12
16	4.243	36	3.830	24	4.123	48	3.109	24
17	4.359	24	4.000	8	4.243	30	3.162	12
18	4.472	24	4.123	48	4.359	72	3.215	12
19	4.583	48	4.163	24	4.472	24	3.266	2
20	4.690	24	4.320	48	4.583	48	3.317	12
21	4.899	24	4.435	72	4.690	24	3.367	6
22	5.000	30	4.619	6	4.796	48	3.416	24
23	5.099	72			4.899	8	3.464	6

TABLE III. Atomization energy/atom, $\Delta E(n)/n$, for spherical clusters (M_n) having cubic lattices. Energies are in hu.

shell number	sc		bcc		fcc	
	n	$\Delta E(n)/n$	n	$\Delta E(n)/n$	n	$\Delta E(n)/n$
0	1	0.0000	1	0.0000	1	0.0000
1	7	0.6999	9	0.6285	13	1.8462
2	19	1.3232	15	1.3963	19	1.9022
3	27	1.5713	27	1.3205	43	2.0163
4	33	1.4758	51	1.5501	55	2.0885
5	57	1.4597	59	1.6416	79	2.2039
6	81	1.7090	65	1.7025	87	2.1685
7	93	1.6567	89	1.5713	135	2.2385
8	123	1.7149	113	1.7196	141	2.2346
9	147	1.7048	137	1.7143	177	2.2746
10	171	1.7464	169	1.8045	201	2.3221
11	179	1.7726	181	1.7715	225	2.3010
12	203	1.7254	229	1.7562	249	2.3103
13	251	1.7977	259	1.8083	321	2.3464
14	257	1.7739	283	1.8400	369	2.3662
15	305	1.7823	307	1.8282	381	2.3687
16	341	1.7943	331	1.8471	429	2.3660
17	365	1.8162	339	1.8529	459	2.3653
18	389	1.8024	387	1.8389	531	2.3805
19	437	1.8186	411	1.8614	555	2.3902
20	461	1.8403	459	1.8407		
21	485	1.8472	531	1.8801		
22	515	1.8222	537	1.8850		
∞	∞	2.0048	∞	2.0641	∞	2.6168

TABLE IV. Liquid drop A and B parameters for clusters having cubic lattice structures.[41] Comparison of extrapolated and "exact" bulk cohesive energies.

	-A		B
	Eq. (8)	Eq. (15)	Eq. (15)
sc	2.00	2.18(4)	2.5(2)
bcc	2.06	2.26(5)	2.8(2)
fcc	2.62	2.61(1)	1.90(6)

TABLE V. Fermi level degeneracy, $D_n(0)$, for bcc clusters and Fermi energy (E_f in hu) of fcc clusters. For sc and bcc structures, $E_f = 0$.

shell number	bcc			fcc	
	n	$D_n(0)$	$D_n(0)/n$	n	E_f
0	1	1	1.000	1	0.000
1	9	7	0.778	13	0.000
2	15	7	0.467	19	0.000
3	27	13	0.481	43	0.867
4	51	19	0.373	55	1.000
5	59	19	0.322	79	0.648
6	65	19	0.292	87	0.664
7	89	31	0.348	135	0.586
8	113	31	0.274	141	0.618
9	137	37	0.270	177	0.673
10	169	37	0.219	201	0.826
11	181	43	0.238	225	0.588
12	229	55	0.240	249	0.893
13	259	55	0.212	321	0.860
14	283	55	0.194	369	0.881
15	307	61	0.199	381	0.910
16	331	61	0.184	429	0.770
17	339	61	0.180	459	0.814
18	387	73	0.189	531	0.805
19	411	73	0.178	555	0.839
20	459	85	0.185		
21	531	85	0.160		
22	537	85	0.158		
∞	∞	∞	0.000	∞	0.459

FIGURE CAPTIONS

Fig. 1. Atomization energy per atom for bcc, fcc and most stable M_2-M_{14} clusters (from Refs. 27, 28; data points omitted for clarity). Full lines pertain to a liquid drop model.

Fig. 2. Hückel eigenvalues $\varepsilon(n)$ for spherical clusters containing up to 500-600 atoms. Energy levels are denoted by horizontal tic marks. Orbital degeneracies are omitted for clarity.

Fig. 3. Density of state profiles for small clusters and comparison with the bulk. Cluster $g_n(\varepsilon)$ pertain to the total number of states within an energy increment $\Delta\varepsilon$ = 0.4848 hu (see text). For $n = \infty$, $g(\varepsilon)$ is the DOS per unit volume obtained from a tight binding calculation. The arrows in Fig. 3(c) denote the Fermi energy (E_f).

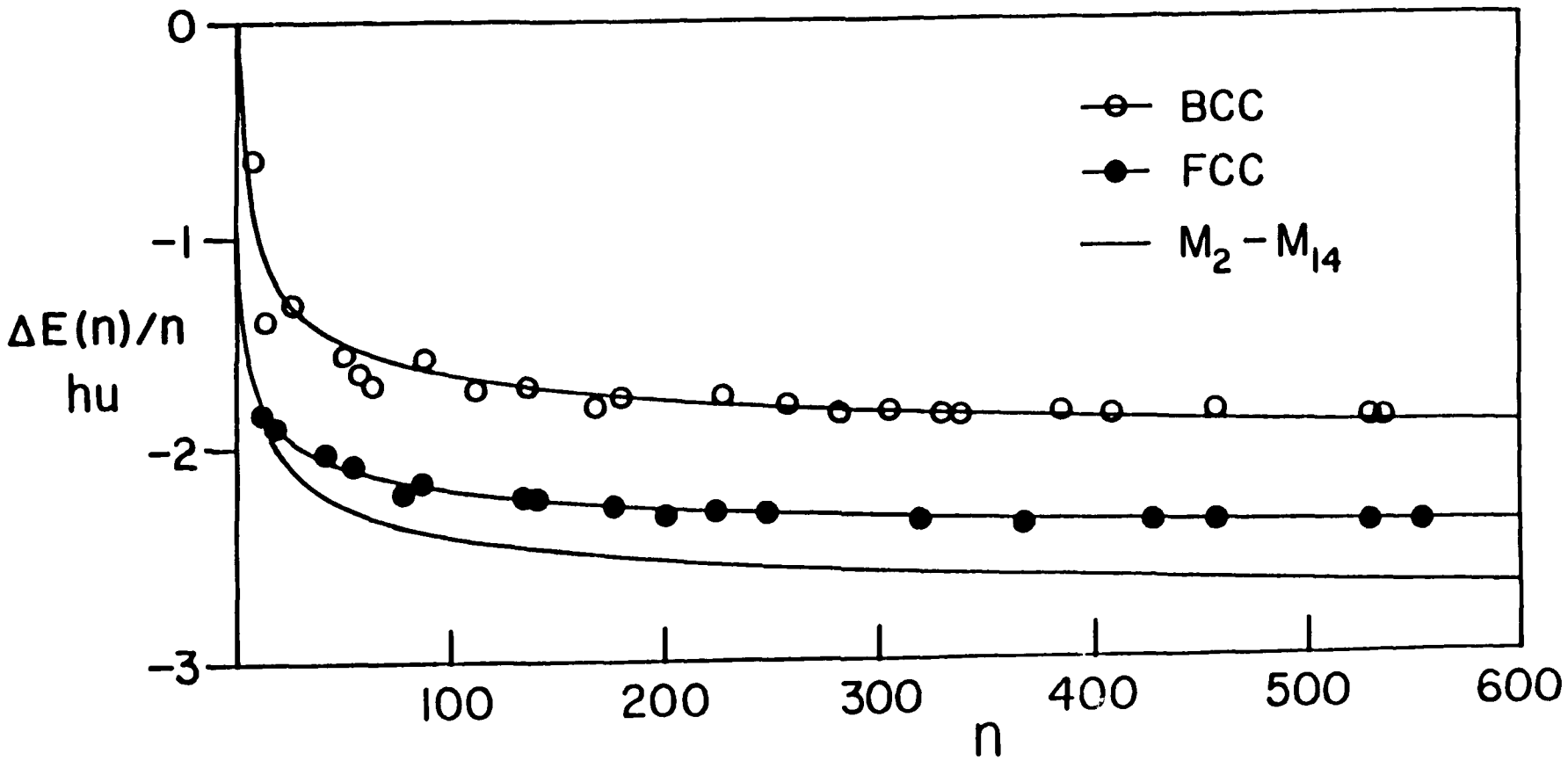

FIG. 1

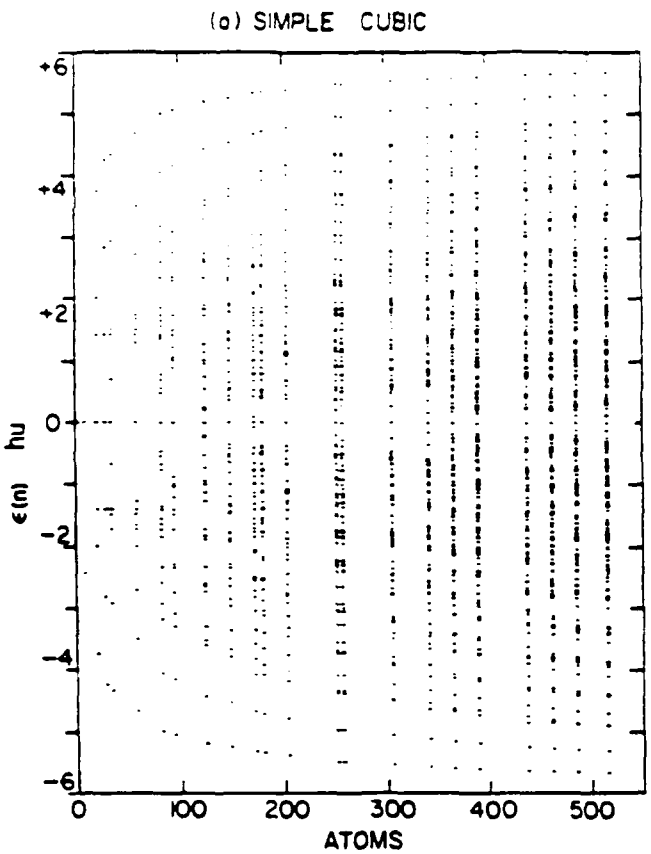
(a) SIMPLE CUBIC
+6
+4
+2
0
-2
-4
-6
ε(n) hu
0
100
200
300
400
500
ATOMS

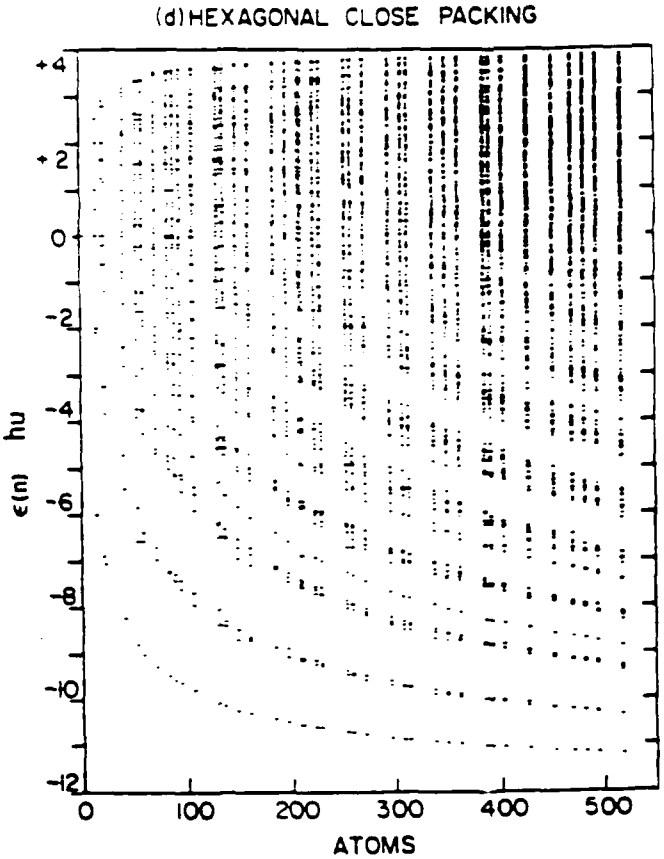
(d) HEXAGONAL CLOSE PACKING
+4
+2
0
-2
-4
-6
-8
-10
-12
ε(n) hu
0
100
200
300
400
500
ATOMS

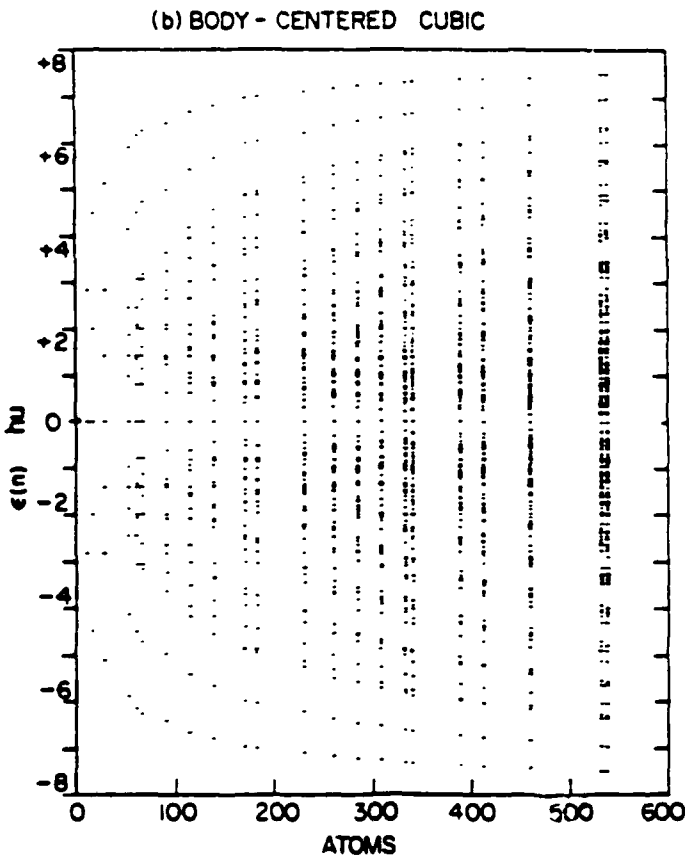
(b) BODY - CENTERED CUBIC
+8
+6
+4
+2
0
-2
-4
-6
-8
ε(n) hu
0
100
200
300
400
500
600
ATOMS

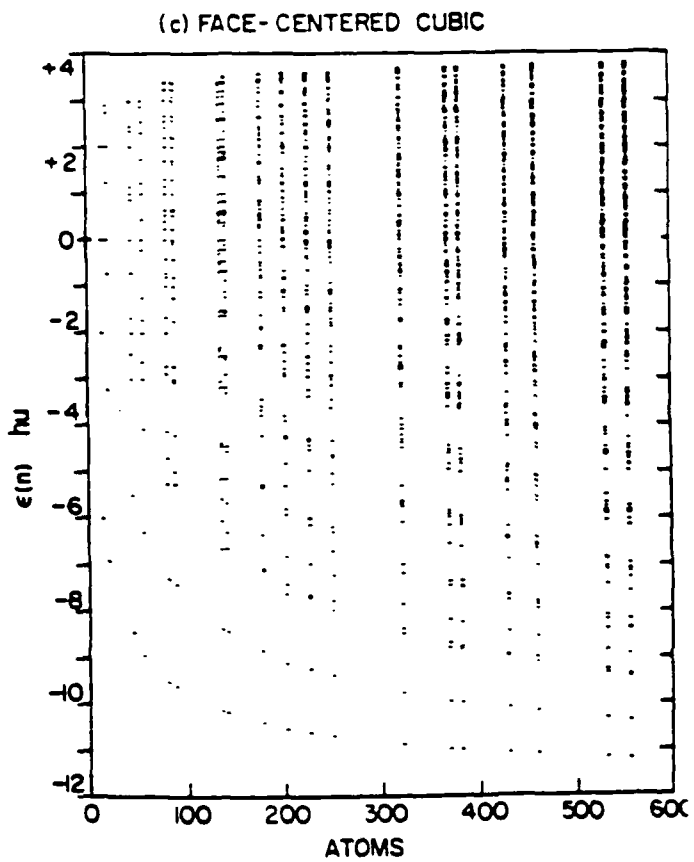
(c) FACE - CENTERED CUBIC
+4
+2
0
-2
-4
-6
-8
-10
-12
ε(n) hu
0
100
200
300
400
500
600
ATOMS

FIG. 2

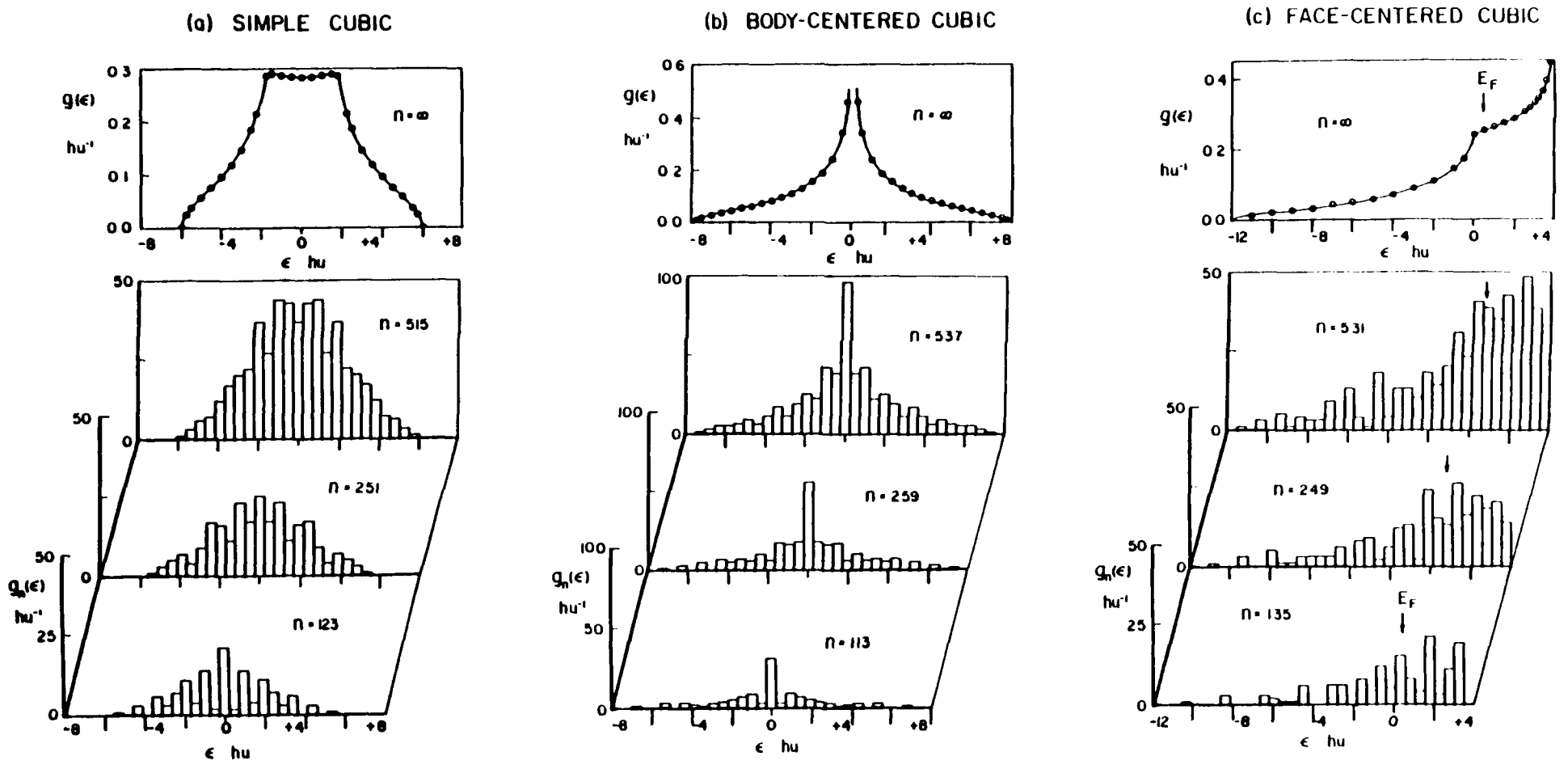
(a) SIMPLE CUBIC
(b) BODY-CENTERED CUBIC
(c) FACE-CENTERED CUBIC
g(ϵ)
hu⁻¹
n = ∞
ϵ hu
n = 515
n = 251
n = 123
n = 537
n = 259
n = 113
n = 531
n = 249
n = 135
E_F
g_n(ϵ)

FIG. 3

TECHNICAL REPORT DISTRIBUTION LIST, GEN

	No. Copies
Office of Naval Research Attn: Code 1113 800 N. Quincy Street Arlington, Virginia 22217-5000	2
Dr. Bernard Douda Naval Weapons Support Center Code 50C Crane, Indiana 47522-5050	1
Naval Civil Engineering Laboratory Attn: Dr. R. W. Drisko, Code L52 Port Hueneme, California 93401	1
Defense Technical Information Center Building 5, Cameron Station Alexandria, Virginia 22314	12 high quality
DTNSRDC Attn: Dr. H. Singerman Applied Chemistry Division Annapolis, Maryland 21401	1
Dr. William Tolles Superintendent Chemistry Division, Code 6100 Naval Research Laboratory Washington, D.C. 20375-5000	1
Dr. David Young Code 334 NORDA NSTL, Mississippi 39529	1
Naval Weapons Center Attn: Dr. Ron Atkins Chemistry Division China Lake, California 93555	1
Scientific Advisor Commandant of the Marine Corps Code RD-1 Washington, D.C. 20380	1
U.S. Army Research Office Attn: CRD-AA-IP P.O. Box 12211 Research Triangle Park, NC 27709	1
Mr. John Boyle Materials Branch Naval Ship Engineering Center Philadelphia, Pennsylvania 19112	1
Naval Ocean Systems Center Attn: Dr. S. Yamamoto Marine Sciences Division San Diego, California 91232	1
Dr. David L. Nelson Chemistry Division Office of Naval Research 800 North Quincy Street Arlington, Virginia 22217	1

ABSTRACTS DISTRIBUTION LIST, 056/625/629

Dr. J. E. Jensen
Hughes Research Laboratory
3011 Malibu Canyon Road
Malibu, California 90265

Dr. J. H. Weaver
Department of Chemical Engineering
and Materials Science
University of Minnesota
Minneapolis, Minnesota 55455

Dr. A. Reisman
Microelectronics Center of North Carolina
Research Triangle Park, North Carolina
27709

Dr. M. Grunze
Laboratory for Surface Science and
Technology
University of Maine
Orono, Maine 04469

Dr. J. Butler
Naval Research Laboratory
Code 6115
Washington D.C. 20375-5000

Dr. L. Interante
Chemistry Department
Rensselaer Polytechnic Institute
Troy, New York 12181

Dr. Irvin Heard
Chemistry and Physics Department
Lincoln University
Lincoln University, Pennsylvania 19352

Dr. K.J. Klaubunde
Department of Chemistry
Kansas State University
Manhattan, Kansas 66506

Dr. C. B. Harris
Department of Chemistry
University of California
Berkeley, California 94720

Dr. F. Kutzler
Department of Chemistry
Box 5055
Tennessee Technological University
Cookesville, Tennessee 38501

Dr. D. DiLella
Chemistry Department
George Washington University
Washington D.C. 20052

Dr. R. Reeves
Chemistry Department
Renssaeler Polytechnic Institute
Troy, New York 12181

Dr. Steven M. George
Stanford University
Department of Chemistry
Stanford, CA 94305

Dr. Mark Johnson
Yale University
Department of Chemistry
New Haven, CT 06511-8118

Dr. W. Knauer
Hughes Research Laboratory
3011 Malibu Canyon Road
Malibu, California 90265

ABSTRACTS DISTRIBUTION LIST, 056/625/629

Dr. G. A. Somorjai
Department of Chemistry
University of California
Berkeley, California 94720

Dr. J. Murday
Naval Research Laboratory
Code 6170
Washington, D.C. 20375-5000

Dr. J. B. Hudson
Materials Division
Rensselaer Polytechnic Institute
Troy, New York 12181

Dr. Theodore E. Madey
Surface Chemistry Section
Department of Commerce
National Bureau of Standards
Washington, D.C. 20234

Dr. J. E. Demuth
IBM Corporation
Thomas J. Watson Research Center
P.O. Box 218
Yorktown Heights, New York 10598

Dr. M. G. Lagally
Department of Metallurgical
and Mining Engineering
University of Wisconsin
Madison, Wisconsin 53706

Dr. R. P. Van Duyne
Chemistry Department
Northwestern University
Evanston, Illinois 60637

Dr. J. M. White
Department of Chemistry
University of Texas
Austin, Texas 78712

Dr. D. E. Harrison
Department of Physics
Naval Postgraduate School
Monterey, California 93940

Dr. R. L. Park
Director, Center of Materials
Research
University of Maryland
College Park, Maryland 20742

Dr. W. T. Peria
Electrical Engineering Department
University of Minnesota
Minneapolis, Minnesota 55455

Dr. Keith H. Johnson
Department of Metallurgy and
Materials Science
Massachusetts Institute of Technology
Cambridge, Massachusetts 02139

Dr. S. Sibener
Department of Chemistry
James Franck Institute
5640 Ellis Avenue
Chicago, Illinois 60637

Dr. Arnold Green
Quantum Surface Dynamics Branch
Code 3817
Naval Weapons Center
China Lake, California 93555

Dr. A. Wold
Department of Chemistry
Brown University
Providence, Rhode Island 02912

Dr. S. L. Bernasek
Department of Chemistry
Princeton University
Princeton, New Jersey 08544

Dr. W. Kohn
Department of Physics
University of California, San Diego
La Jolla, California 92037

ABSTRACTS DISTRIBUTION LIST, 056/625/629

Dr. F. Carter
Code 6170
Naval Research Laboratory
Washington, D.C. 20375-5000

Dr. Richard Colton
Code 6170
Naval Research Laboratory
Washington, D.C. 20375-5000

Dr. Dan Pierce
National Bureau of Standards
Optical Physics Division
Washington, D.C. 20234

Dr. R. Stanley Williams
Department of Chemistry
University of California
Los Angeles, California 90024

Dr. R. P. Messmer
Materials Characterization Lab.
General Electric Company
Schenectady, New York 22217

Dr. Robert Gomer
Department of Chemistry
James Franck Institute
5640 Ellis Avenue
Chicago, Illinois 60637

Dr. Ronald Lee
R301
Naval Surface Weapons Center
White Oak
Silver Spring, Maryland 20910

Dr. Paul Schoen
Code 6190
Naval Research Laboratory
Washington, D.C. 20375-5000

Dr. John T. Yates
Department of Chemistry
University of Pittsburgh
Pittsburgh, Pennsylvania 15260

Dr. Richard Greene
Code 5230
Naval Research Laboratory
Washington, D.C. 20375-5000

Dr. L. Kesmodel
Department of Physics
Indiana University
Bloomington, Indiana 47403

Dr. K. C. Janda
University of Pittsburg
Chemistry Building
Pittsburg, PA 15260

Dr. E. A. Irene
Department of Chemistry
University of North Carolina
Chapel Hill, North Carolina 27514

Dr. Adam Heller
Bell Laboratories
Murray Hill, New Jersey 07974

Dr. Martin Fleischmann
Department of Chemistry
University of Southampton
Southampton 509 5NH
UNITED KINGDOM

Dr. H. Tachikawa
Chemistry Department
Jackson State University
Jackson, Mississippi 39217

Dr. John W. Wilkins
Cornell University
Laboratory of Atomic and
Solid State Physics
Ithaca, New York 14853

ABSTRACTS DISTRIBUTION LIST, 056/625/629

Dr. R. G. Wallis
Department of Physics
University of California
Irvine, California 92664

Dr. D. Ramaker
Chemistry Department
George Washington University
Washington, D.C. 20052

Dr. J. C. Hemminger
Chemistry Department
University of California
Irvine, California 92717

Dr. T. F. George
Chemistry Department
University of Rochester
Rochester, New York 14627

Dr. G. Rubloff
IBM
Thomas J. Watson Research Center
P.O. Box 218
Yorktown Heights, New York 10598

Dr. Horia Metiu
Chemistry Department
University of California
Santa Barbara, California 93106

Dr. W. Goddard
Department of Chemistry and Chemical
Engineering
California Institute of Technology
Pasadena, California 91125

Dr. P. Hansma
Department of Physics
University of California
Santa Barbara, California 93106

Dr. J. Baldeschwieler
Department of Chemistry and
Chemical Engineering
California Institute of Technology
Pasadena, California 91125

Dr. J. T. Keiser
Department of Chemistry
University of Richmond
Richmond, Virginia 23173

Dr. R. W. Plummer
Department of Physics
University of Pennsylvania
Philadelphia, Pennsylvania 19104

Dr. E. Yeager
Department of Chemistry
Case Western Reserve University
Cleveland, Ohio 41106

Dr. N. Winograd
Department of Chemistry
Pennsylvania State University
University Park, Pennsylvania 16802

Dr. Roald Hoffmann
Department of Chemistry
Cornell University
Ithaca, New York 14853

Dr. A. Steckl
Department of Electrical and
Systems Engineering
Rensselaer Polytechnic Institute
Troy, NewYork 12181

Dr. G.H. Morrison
Department of Chemistry
Cornell University
Ithaca, New York 14853